

RESEARCH

Open Access



Transcriptome sequencing–based analysis of the molecular mechanism underlying the effect of lncRNA AC003090.1 on osteoporosis

Huafeng Zhuang^{1,2}, Yongjun Lin², Chengye Lin², Miao Zheng³, Yizhong Li², Xuedong Yao^{2*} and Youjia Xu^{1,3*}

Abstract

Objective To analyze changes in the expression of osteoporosis (OP)-related genes across different bone types based on transcriptome sequencing, and to identify the key molecules and mechanisms involved in the progression of OP in order to better understand this process.

Methods Ten pairs of postmenopausal patients with osteoporosis (OP) and non-osteoporotic (non-OP) volunteers were included. Transcriptome sequencing was performed on six pairs of spongy and cortical bone tissues. The expression of FOXP1 was detected using quantitative real-time PCR (RT-qPCR) and receiver operating characteristic (ROC) curves. Magnetic-activated cell sorting was conducted, and the expression levels of AC003090.1, miR-203a-3p, and FOXP1 were measured using RT-qPCR. Human bone marrow stem cells (hBMSCs) were infected with a lentivirus carrying the AC003090.1 expression plasmid. The expression levels of Runx2, Opn, and Ocn in spongy and cortical bone samples, as well as in post-infection cells, were assessed through RT-qPCR. The expression levels of GSK-3 β , β -catenin, and c-Myc were evaluated by performing RT-qPCR and Western blot analysis.

Result A total of 2,102 out of 2,827 differentially expressed genes (DEGs) were identified between the cortical bone samples from patients with osteoporosis (OP) and the cortical/spongy bone samples of the control group. Among these, 1,482 were significantly up-regulated, and 620 were significantly down-regulated, while 1,146 were significantly up-regulated and 1,681 were significantly down-regulated. The expression of FOXP1 in tissue and bone tissue-derived mesenchymal stem cells (MSCs) from patients with OP was significantly lower than that in patients without OP. FOXP1 levels in bone tissue (cortical bone AUC=0.825, $P=0.01405$; spongy bone AUC=0.800, $P=0.02338$) could serve as predictors of OP. In addition, the overexpression of AC003090.1 significantly enhanced the transcription levels of Runx2, Opn, and Ocn; significantly upregulated the expression levels of β -catenin and c-Myc; and inhibited the expression of GSK-3 β . Transfection with miR-203a-3p mimics and FOXP1 small interfering RNA reversed the effect of AC003090.1 on GSK-3 β / β -catenin/c-Myc signaling.

Conclusion FOXP1, as a molecular mediator of AC003090.1, affects the GSK-3 β / β -catenin/c-Myc signaling pathway and promotes the osteogenic differentiation of hBMSCs, thus playing a key role in the progression of OP.

*Correspondence:

Xuedong Yao
yaodoctor2013@126.com
Youjia Xu
xuyoujia@edu.suda.cn

Full list of author information is available at the end of the article



© The Author(s) 2025. **Open Access** This article is licensed under a Creative Commons Attribution-NonCommercial-NoDerivatives 4.0 International License, which permits any non-commercial use, sharing, distribution and reproduction in any medium or format, as long as you give appropriate credit to the original author(s) and the source, provide a link to the Creative Commons licence, and indicate if you modified the licensed material. You do not have permission under this licence to share adapted material derived from this article or parts of it. The images or other third party material in this article are included in the article's Creative Commons licence, unless indicated otherwise in a credit line to the material. If material is not included in the article's Creative Commons licence and your intended use is not permitted by statutory regulation or exceeds the permitted use, you will need to obtain permission directly from the copyright holder. To view a copy of this licence, visit <http://creativecommons.org/licenses/by-nc-nd/4.0/>.

Keywords Transcriptome sequencing, Osteoporosis, AC003090.1, Mesenchymal stem cells, Osteogenic differentiation

Introduction

Osteoporosis (OP) is a serious systemic metabolic bone disease. It is characterised by decreased bone mass and changes in bone microstructure accompanied with reduced bone strength and increased bone fragility and fracture risk [1, 2, 3]. The pathogenesis of OP has been preliminarily clarified as follows: the dynamic balance of bone reconstruction is destroyed, and the functions of osteoblasts and osteoclasts are unbalanced, resulting in the imbalance of bone metabolism and loss of net bone volume [4, 5]. Drugs, such as bisphosphonate calcitonin, which are widely used in clinical practice, mainly decelerate the development of OP through antbone resorption but cannot markedly improve the microstructure of bone trabeculae [6]. Therefore, improving bone formation ability has become the focus of OP treatment [7, 8, 9].

Bone marrow mesenchymal stem cells (BMSCs), the precursors of osteoblasts, have weak osteogenic differentiation ability, which has been proven to be the main cytological basis of the pathogenesis of OP, and can directly participate in the occurrence and development of OP [10, 11]. Osteoblast differentiation is regulated by various hormone cytokines, such as TGF-1/2, VEGF and FGF2. In recent years, a large number of studies have shown that BMSCs can differentiate into osteoblasts under certain environmental induction. Moreover, BMSCs have become a type of seed cells that are expected to participate in the clinical treatment of OP due to their characteristics of easy extraction and isolation and considerable proliferation *in vitro*. Studies have also demonstrated that the osteogenic differentiation ability of BMSCs is closely related to the expression of certain genes (FOXP1, Osterix, GLP-1R, Nrf2 and DLX2) [12, 13, 14, 15, 16]. FOXP1 is one of four FOXP subfamily members (FOXP1, FOXP2, FOXP3 and FOXP4); it is widely expressed in diverse tissues and cells of mammals and controls and determines the differentiation and fate of various cells [17]. For example, in *Foxp1* knockout mice, defects in cardiomyocyte maturation and proliferation resulted in severe defects in cardiac morphogenesis and embryo death [18]. In developing embryonic and postnatal lung secretory epithelial cells, the absence of *Foxp1/4* led to the abnormal activation of secretory epithelial cells to differentiate into goblet cells [19].

In recent years, with the continuous development of high-throughput sequencing technology and interdisciplinary and multidisciplinary methods, a growing number of studies have shown that lncRNAs participate in complex signalling networks in human cells, as well as regulate gene expression and cell proliferation and differentiation in response to various stimuli and signals

[20, 21, 22]. lncRNAs can participate in the regulation of BMSCs [23] and osteoblast activity [24], thus remarkably affecting bone metabolism. Our previous study [25] illustrated that AC003090.1 is a novel lncRNA with an important role in the osteogenic differentiation of human BMSCs (hBMSCs). The overexpression of AC003090.1 remarkably promoted the osteogenic differentiation of hBMSCs *in vitro*. The gene editing of hBMSCs targeting lncRNA AC003090.1 may be beneficial to the clinical application of MSCs. In our previous study, we identified the key role of the lncRNA AC003090.1/miR-203a-3p/FOXP1 axis in the osteogenic differentiation of hBMSCs and progression of OP. However, the molecular mechanism involved in its biological function still needs further exploration.

By analysing transcriptomic expression profiles, we provided the direction for exploring the downstream signalling of the lncRNA AC003090.1/miR-203a-3p/FOXP1 axis and verified it at the clinical and cellular levels to further reveal the mechanism through which lncRNA AC003090.1 affects OP osteogenic differentiation.

Materials and methods

Patient samples

This study included cortical and spongy bone samples from 20 postmenopausal women who underwent hip replacement surgery for hip diseases in the Second Affiliated Hospital of Fujian Medical University in 2021. The inclusion criteria were as follows: (1) With and without OP diagnosed in accordance with the 2017 Chinese Guidelines for the Diagnosis and Treatment of Primary Osteoporosis. (2) No serious liver, kidney and thyroid diseases; malignant tumours; and history of major disease. Exclusion criteria: (1) Treated with anti-OP drugs before surgery. (2) Long-term use of monoclonal antibodies and other drugs affecting bone differentiation. (3) Hip fracture from severe violent trauma, such as car accidents, falling from heights and injuries from heavy objects. (4) Pathological fracture.

Cell culture and transfection

hBMSCs were obtained from BeNa Culture Collection (BNCC339828, China) and cultured in OriCell™ hBMSC complete culture medium (BGM-0111, Cyagen Biosciences, China) composed of 10% special foetal bovine serum (10099-141, Gibco, the USA), 1% penicillin and streptomycin solution (100×, C0222, Beytime, China) and 1% glutamine (C0221, Beytime, China). The medium was changed every 2–3 days, and cells were grown to approximately 80% confluence. Subculture was conducted with a 1:3 ratio at 37 °C in a 5% CO₂ cell incubator. miR-203a-3p

mimics/NC and small-interfering RNA (siRNA) for FOXP1 were synthesised by General Biol (Anhui, China). The recombinant overexpression plasmid for lncRNA AC003090.1 was established in pLVX-mcmv-ZsGreen1-puro (expressed as oelnc/oelnc NC). hBMSCs were transfected by using Invitrogen Lipofectamine™ 2000 (transfection reagent [μ L]: plasmid [μ g] = 3:1), and the transfection solution was changed 12 h after transfection.

RNA isolation and quantitative real-time qPCR

A TaKaRa MiniBEST Universal RNA extraction kit (9767, Takara, Japan) was employed to obtain total RNA from samples, and a PrimeScript™ II 1st Strand cDNA synthesis kit (6210 A, Takara, Japan) was applied for cDNA synthesis. lncRNA AC003090.1, miR-203a-3p, FOXP1 and β -catenin expression levels were measured by using AceQ® qPCR SYBR Green Master Mix (Q111-02, Vazyme, China). GAPDH was used as an endogenous control for lncRNA AC003090.1, FOXP1, Runx2, Ocn, GSK3 β , c-Myc and β -catenin. U6 was applied as an endogenous control for miR-203a-3p. All experiments were performed in accordance with kit instructions. Primer sequences are shown in Table 1.

Western blot analysis

Western blot analysis was conducted to detect the expression levels of proteins. Cells were collected, and total protein was obtained. A BCA kit was used to detect protein concentration. Samples were separated through SDS-PAGE; transferred onto a nitrocellulose filter membrane; and incubated with GSK3 β rabbit mAb (cat no. A11731, 1:1000), c-Myc rabbit mAb (cat no. A19032, 1:1000) and β -catenin mouse mAb (cat no. A20221, 1:1000) at 4 °C overnight and with secondary antibodies for 1 h. Finally, an ECL detection system was used to detect bands. GAPDH was used as an endogenous control.

Magnetic activated cell sorting

Cell suspensions were prepared as follows: spongy and cortical bone tissues from the OP ($n=6$) and control ($n=6$) groups were cut in PBS into fragments of approximately 1 mm³. Bone tissue fragments and cells inoculated at a density of 1×10^9 L⁻¹ were sequentially digested with 2 g/L type II collagenase and 2.5 g/L trypsin. When primary cells had fused and covered more than 80% of the bottom of the bottle, they were digested with 2.5 g/L trypsin to obtain a cell suspension.

Fluorescein-labelled CD166/CD105 antibodies were added to the prepared cell suspension. Incubation, isolation and collection were repeated, and the resulting CD105⁺/CD166⁺ cell suspension was used as the cells for magnetic activated cell sorting (MACS). The cells collected as the fluid without magnetic beads were mixed with non-CD105⁺/CD166⁺ cells as a control.

RNA-seq

A TaKaRa MiniBEST Universal RNA extraction kit (9767, Takara, Japan) was used to obtain total RNA from samples (spongy and cortical bone tissues of the OP [$n=6$] and control [$n=6$] groups). Paired-end sequencing was performed by using next-generation sequencing (NGS) with an Illumina HiSeq sequencing platform. The reference genome employed in this project was GCF-000001405.39-GRCh38.p13-genomic.fna.

Statistical analysis

Statistical analyses were conducted with SPSS 20.0 statistical software. Unpaired two-sided t-test was used to analyse statistical differences between groups. Data were expressed as mean \pm SD. ROC curves were obtained through analysis with GraphPad Prism6. $P < 0.05$ was employed to indicate biostatistical significance.

HTSeq was applied for the statistical comparison of the read count value of each gene as the original expression of the gene [26]. FPKM values were calculated by using

Table 1 Sequences

Gene	Forward	Reverse
GAPDH	AGAAGGCTGGGGCTCATTG	AGGGGCCATCCACAGTCTTC
U6	CTCGCTTCGGCAGCACA	AACGCTTCACGAATTTGCGT
lncRNA AC003090.1	CTGCCTGCTTTGTTTACACGAA	TGTTGCCGAGTCAATCATTAT
hsa-miR-203a-3p	GCGGCGGGTGAAATGTTTAGGAC	ATCCAGTGCAGGGTCCGAGG
FOXP1	GCAGTTACAGCAGCAGCACCTCC	CAGCCTGGCCACTTGCATACACC
β -catenin	AAGCGGCTGTTAGTCACTGG	CGAGTCATTGCATACTGTCCAT
GSK3 β	TGTGTGTTGGCTGAGCTGTT	CTCCCTTGTGGAGTTCGCCAG
c-myc	CCTACCCTCTCAACGACAGC	TTGTTCTCTCAGAGTCGC
RUNX2	CACCACTACTACCACACCTA	TGACGAAGTGCCATAGTAGAGAT
OCN	CACACTCCTCGCCCTATTG	GGTCTCTTCACTACCTCGCT
OPN	GAAGTTTCGCAGACCTGACAT	GTATGCACCACTCACTCCTCG

GAPDH: glyceraldehyde-3-phosphate dehydrogenase; FOXP1: Forkhead Box P1; GSK3 β : Recombinant Glycogen Synthase Kinase 3 Beta; Runx2: Runt-related transcription factor 2; OCN: Osteocalcin; OPN: Osteocalcin

Stringtie and TMM [27]. The DESeq software package in R language was employed for the PCA of each sample in accordance with expression levels. The screening criteria for DEGs were $|\log_2\text{FoldChange}| > 1$ and $P < 0.05$.

The R language ggplots2 software package was used to draw the volcano map of DEGs. The R Circlize software package was utilised to label DEGs in the genome. The Pheatmap software package in R language was utilised for bidirectional cluster analysis. topGO was employed for GO enrichment analysis, and the phyper function in R software was applied for KEGG enrichment analysis.

Results

Statistical and characteristic analyses of gene expression levels in each sample

FPKM values were used to characterise gene expression levels, and each sequenced sample was statistically analysed ('A' represents the spongy bone samples of patients with OP, 'aa' represents the cortical bone samples of patients with OP, 'B' represents the spongy bone samples of the control group and 'bb' represents the cortical bone samples of the control group). Each group contained six samples, and the number represents the number of genes in different FPKM value intervals (different expression level intervals). Fragments refer to each nucleic acid fragment used for sequencing. In our study, genes with $\text{FPKM} > 1$ were considered as expressed.

FPKM density (Fig. 1A) and violin (Fig. 1B) maps were drawn to display the number of genes with different expression levels in all samples intuitively. The FPKM density and violin maps showed the gene expression characteristics of each sample: the majority of genes exhibited medium expression levels, and a few genes presented very high or low expression levels. The characteristics of gene expression in all samples were consistent, as shown in Table 2.

DEG analysis

In our study, the genes expressed in different groups were compared in pairs, namely, aa vs. bb, A vs. aa, A vs. B and B vs. bb. A volcano map of gene distribution, multiple differences in gene expression and significant results between the two groups was drawn, as presented in Fig. 1C, to display the DEG data of the two groups directly. A total of 2102 DEGs were obtained between groups aa vs. bb. Of these DEGs, 1482 were significantly up-regulated and 620 were significantly down-regulated. A total of 667 DEGs were obtained between groups A and aa, of which 305 were significantly up-regulated and 362 were significantly down-regulated. A total of 2827 DEGs were obtained between groups A and B, with 1681 and 1146 of these DEGs being significantly up-regulated and significantly down-regulated, respectively. A total of 2156 DEGs were obtained between groups B and bb. Of

these DEGs, 1234 were significantly up-regulated and 922 were significantly down-regulated. In addition, we ranked the genes with up-regulated and down-regulated expression levels in accordance with FC values. The top 20 genes in each ranking are listed in Table 3.

Cluster analysis of DEGs

Figure 1D shows the results of bidirectional cluster analysis, which was conducted in accordance with the expression levels of the same gene in different samples and expression patterns of different genes in the same sample. In this figure, genes are represented horizontally, with red representing those with high expression and green representing those with low expression.

GO enrichment analysis of DEGs

As illustrated in Fig. 2A, we used the rich factor, false discovery rate (FDR) and number of genes enriched in GO items to measure the enrichment degree of each GO item further. FDR generally ranges from 0 to 1. An FDR value close to zero is indicative of significant enrichment. Amongst all the items, the first 20 items with the smallest FDR values, that is, the most significant enrichment, were selected for display. Numerous items were correlated with 'extracellular components', 'cell localisation', 'cell movement', 'cell adhesion', 'anatomical structure development', 'phylogeny', 'animal organ development', 'multicellular organ development' and 'skeletal system development'.

KEGG enrichment analysis of DEGs

The KEGG pathway database includes cellular processes, environmental information processing, genetic information processing, human diseases, metabolism and organismal systems. In this study, the DEGs enriched in the entries obtained through comparison amongst different groups were counted in accordance with the second-level entries of the KEGG pathway database. The enrichment degree of each KEGG pathway was measured by using the rich factor, FDR and number of genes enriched in KEGG pathways. The first 20 pathways with the smallest FDR value, that is, the most significant enrichment, amongst all the pathways were selected for display in Fig. 2B.

Role of FOXP1 in OP

Figure 3B shows that the expression of FOXP1 in the bone tissue of patients with OP was significantly down-regulated relative to that in control patients. The expression pattern of FOXP1 in the bone tissue of patients with OP obtained through high-throughput transcriptome sequencing (Fig. 3A) was consistent with that in patients with OP detected by using quantitative real-time PCR (RT-qPCR).

Table 2 Statistical table of interval distribution of sample expression

Type	0 ~ 0.01	0.01 ~ 0.1	0.1 ~ 1	1 ~ 10	10 ~ 100	100 ~ 1000	> 1000
A35	6372 (28.56%)	1617 (7.25%)	3346 (15%)	6571 (29.45%)	3851 (17.26%)	496 (2.22%)	59 (0.26%)
A36	6229 (27.92%)	1592 (7.14%)	3219 (14.43%)	6542 (29.32%)	4169 (18.69%)	509 (2.28%)	52 (0.23%)
A29	6304 (28.25%)	1578 (7.07%)	3093 (13.86%)	6698 (30.02%)	4131 (18.51%)	467 (2.09%)	41 (0.18%)
A31	6672 (29.9%)	1423 (6.38%)	3086 (13.83%)	6491 (29.09%)	4076 (18.27%)	505 (2.26%)	59 (0.26%)
A32	6374 (28.57%)	1513 (6.78%)	3185 (14.27%)	6505 (29.15%)	4193 (18.79%)	492 (2.21%)	50 (0.22%)
A34	6131 (27.48%)	1739 (7.79%)	3255 (14.59%)	6545 (29.33%)	4072 (18.25%)	516 (2.31%)	54 (0.24%)
aa29	6127 (27.46%)	1791 (8.03%)	3225 (14.45%)	6611 (29.63%)	4041 (18.11%)	473 (2.12%)	44 (0.20%)
aa30	6106 (27.37%)	1730 (7.75%)	3171 (14.21%)	6653 (29.82%)	4136 (18.54%)	476 (2.13%)	40 (0.18%)
aa35	6213 (27.85%)	1789 (8.02%)	3240 (14.52%)	6580 (29.49%)	3962 (17.76%)	469 (2.1%)	59 (0.26%)
aa36	5973 (26.77%)	1633 (7.32%)	3284 (14.72%)	6719 (30.11%)	4125 (18.49%)	514 (2.3%)	64 (0.29%)
aa37	6396 (28.67%)	1638 (7.34%)	3357 (15.05%)	6456 (28.94%)	3874 (17.36%)	516 (2.31%)	75 (0.34%)
aa38	6483 (29.06%)	1454 (6.52%)	3433 (15.39%)	6340 (28.42%)	4017 (18%)	516 (2.31%)	69 (0.31%)
B43	6181 (27.7%)	1358 (6.09%)	3064 (13.73%)	6748 (30.24%)	4396 (19.7%)	515 (2.31%)	50 (0.22%)
B44	6648 (29.8%)	1724 (7.73%)	3415 (15.31%)	6218 (27.87%)	3780 (16.94%)	461 (2.07%)	66 (0.3%)
B45	6348 (28.45%)	1689 (7.57%)	3595 (16.11%)	6286 (28.17%)	3850 (17.26%)	479 (2.15%)	65 (0.29%)
B46	6095 (27.32%)	1713 (7.68%)	3854 (17.27%)	6432 (28.83%)	3654 (16.38%)	498 (2.23%)	66 (0.30%)
B47	6225 (27.9%)	1771 (7.94%)	3632 (16.28%)	6320 (28.33%)	3828 (17.16%)	482 (2.16%)	54 (0.24%)
B48	6491 (29.09%)	1795 (8.04%)	3509 (15.73%)	6110 (27.38%)	3880 (17.39%)	467 (2.09%)	60 (0.27%)
bb52	6204 (27.81%)	1326 (5.94%)	3161 (14.17%)	6893 (30.89%)	4184 (18.75%)	486 (2.18%)	58 (0.26%)
bb53	6133 (27.49%)	1304 (5.84%)	3193 (14.31%)	6840 (30.66%)	4303 (19.29%)	493 (2.21%)	46 (0.21%)
bb44	6180 (27.7%)	1515 (6.79%)	3275 (14.68%)	6724 (30.14%)	4101 (18.38%)	459 (2.06%)	58 (0.26%)
bb54	6087 (27.28%)	1230 (5.51%)	3103 (13.91%)	6943 (31.12%)	4394 (19.69%)	503 (2.25%)	52 (0.23%)
bb50	6108 (27.38%)	1533 (6.87%)	3272 (14.66%)	6897 (30.91%)	4009 (17.97%)	436 (1.95%)	57 (0.26%)
bb51	5823 (26.1%)	1492 (6.69%)	3251 (14.57%)	6811 (30.53%)	4393 (19.69%)	495 (2.22%)	47 (0.21%)

A represents spongy bone samples from OP patients, aa represents cortical bone samples from OP patients; B represents spongy bone samples of control group, and bb represents cortical bone samples of control group. Each group contains 6 samples, and the numbers represent different samples

ROC curve analysis of FOXP1 levels in OP bone tissue

Given the promoting effect of FOXP1 on the osteogenic differentiation of hBMSCs in vitro and the significantly low expression of FOXP1 in the cortical and spongy bone tissues of patients with OP, we performed ROC curve analysis to evaluate the sensitivity and specificity of FOXP1 in bone tissue as a predictor of OP, as shown in Fig. 3C. The AUC of cortical bone was 0.825 (95%CI, 0.627–1.022) and that of spongy bone was 0.0.800 (95%CI, 0.603–0.996). These results suggest the potential value of FOXP1 in bone tissue, especially cortical bone, as a predictor of OP.

Specific expression levels of AC003090.1, miR-203a-3p and FOXP1 in bone tissue-derived MSCs in patients with OP

In our study, MSCs were positively labelled with the cell surface marker CD105/CD166 and separated from the cortical and spongy bone tissues of patients in the control and OP groups by using MACS. Total RNA extraction and RT-qPCR were performed on the selected cells.

In MSCs derived from the cortical and spongy bone tissues of patients with OP, the specific expression levels of AC003090.1 and FOXP1 were down-regulated, whereas that of miR-203a-3p was up-regulated (Fig. 3D, E and F). The expression levels of AC003090.1, miR-203a-3p and FOXP1 in non-MSCs (other cells) did not significantly differ from those in cells from different patient-derived sources (OP and control) and from different bone tissue types (spongy and cortical bones) (Fig. 3D, E and F).

Expression pattern-specific changes in miR-203a-3p and FOXP1 during the osteogenic differentiation of hBMSCs in vitro and lncRNA AC003090.1 regulate their expression changes

Subsequently, we utilised RT-qPCR to detect whether lncRNA AC003090.1 could regulate the changes in the expression levels of miR-203a-3p and FOXP1 during the osteogenic differentiation of hBMSCs in vitro. Figure 5A and B illustrate that the overexpression of lncRNA AC003090.1 significantly down-regulated the expression

Table 3 Top 20 DEGs based on FC value

aa VS. bb		A VS. aa		A VS. B		B VS. bb	
Down	Up	Down	Up	Down	Up	Down	Up
TTR	GSTM1	HLA-DRB5	GSTM1	IL11	HLA-DQB1_2	GSTM1	HLA-DQB1_2
HLA-DMA_3	LILRB3	MS4A6E	HLA-A_4	HLA-DRB5	ANGPTL8	SLC7A3	CFB
HLA-C_2	HLA-A_4	POSTN	HLA-C_6	CCL7	HLA-C_5	SLC6A19	B3GNT3
HLA-C_3	CA9	TREM2	LILRB3	GSTM1	HLA-C_2	FAM81B	FAM163B
CTAG2	WNT2	HLA-DRB1	H1-3	CAMK2A	HLA-C_3	OR2L2	CDH12
NUTM2B	MMP10	DCSTAMP	FFAR1	MS4A6E	HLA-DMA_3	SERPINB2	FRMD7
LMO1	H1-3	MMP12	SLC7A3	CXCL5	HLA-C_6	H3C11	EPHA7
HOXC12	CXCL5	MMP7	HLA-DMA	MMP7	SERTM1	FFAR1	OPCML
FREM2	TCAF2	B3GNT3	VPREB1	DAW1	HSPA1B_2	FOXA1	FAM189A1
LYPD2	SPINK1	SPOCD1	LILRA4	WNT2	RNF5_2	NIPAL4	HAPLN1
CPLX3	KCNF1	NOTUM	TFAP2C	FAM83A	PSMB8_3	GJB6	SCRG1
LGI1	CCL20	IHH	CCDC187	SLC6A19	ARL5C	KRT25	MMP13
FGF16	DMBT1	VARS2_1	HLA-C_5	CCL20	COL28A1	DAW1	SLITRK6
SFRP5	MMP3	NRK	TMEM72	HLA-DRB1	SLC6A2	H2BC13	MEPE
COL28A1	XKR9	GFAP	LEFTY1	CGB5	TSPAN8	ATF6B_3	FAM43B
TSPAN8	NME2	ASPHD1	DNTT	SYT13	ERICH4	EREG	EPHA5
FCGBP_1	GPR142	C5orf46	LOC105379752	MARCHF4	SLC38A11	H1-4	PLA2G2A
FRMPD3	IL11	MARCHF4	OVCH1	SDS	FOXO6_1	LILRA6_4	PRSS35
GCOM1	PRG4	MICB_5	SLC32A1	MPP4	EPHA7	ZAR1	GFAP
MC4R	LOC105378148	COL5A1	TUBB_2	SBSN	CRABP1	TEX45	GNG4_1

A represents spongy bone samples from OP patients, aa represents cortical bone samples from OP patients. B represents spongy bone samples of control group, and bb represents cortical bone samples of control group. Each group contained 6 samples

of miR-203a-3p and up-regulated the mRNA level of FOXP1. Importantly, during the osteogenic differentiation of hBMSCs in vitro, the expression of miR-203a-3p was significantly down-regulated and the mRNA level of FOXP1 was significantly up-regulated (hBMSC OI vs. hBMSCs). These results suggest that miR-203a-3p and FOXP1, as well as their expression regulation mechanisms, are involved in the osteoblastic differentiation of hBMSCs in vitro and may play an important role. lncRNA AC003090.1, as a molecular regulatory mechanism of ceRNAs, can specifically bind to miR-203a-3p and cause its level to decrease, thus leading to the up-regulation of FOXP1 mRNA levels.

Changes in the expression levels of Runx2, Opn and Ocn in the bone tissue/hBMSCs of patients with OP

The transcriptional activation of Runx2, Opn and Ocn represents the prophase, early phase and maturation of osteoblasts, respectively. We detected the levels of Runx2, Opn and Ocn in the bone tissue of patients in the control and OP groups by using RT-qPCR. Figure 4A shows that the Runx2, Opn and Ocn transcription levels in the cortical and spongy bone tissues of patients with OP were significantly lower than those in the control group, indicating differences in the number and/or function of osteoblasts and process of bone formation between patients with OP and those with low bone mass. Figure 4B shows that in the control patients, the Runx2, Opn and Ocn transcription levels in spongy bone

tissues were significantly lower than those in cortical bone. However, the transcription levels of Runx2, Opn and Ocn in the bone tissue of patients with OP were low possibly due to bone formation disorders. Therefore, the transcription levels of Runx2, Opn and Ocn in the cortical and spongy bone tissues of patients with OP did not significantly differ.

We detected the levels of Runx2, Opn and Ocn by using RT-qPCR to analyse the effect of AC003090.1 overexpression on the osteogenic differentiation of hBMSCs. The result is provided in Fig. 5C. Compared with those in normal hBMSCs, the transcription levels of Runx2, Opn and Ocn in the OI of hBMSCs had significantly increased, indicating that hBMSCs were undergoing osteogenic differentiation. Lentiviral vector infection with an empty plasmid (hBMSC OI+lnc-NC) did not affect the transcription of Runx2, Opn and Ocn. However, lentiviral infection with the AC003090.1-expressing plasmid, that is, the overexpression of AC003090.1 (hBMSC OI+lnc-OE), significantly up-regulated Runx2, Opn and Ocn transcription levels relative to transfection with hBMSC OI. This result demonstrates that the overexpression of AC003090.1 significantly promoted the osteogenic differentiation of hBMSCs. Figure 6A illustrates that compared with hBMSC OI+lnc-OE transfection, NC transfection did not affect the transcription levels of Runx2, Opn and Ocn. However, compared with hBMSC OI+lnc-OE transfection, transfection with miR-203a-3p mimics and si-FOXP1, especially si-FOXP1,

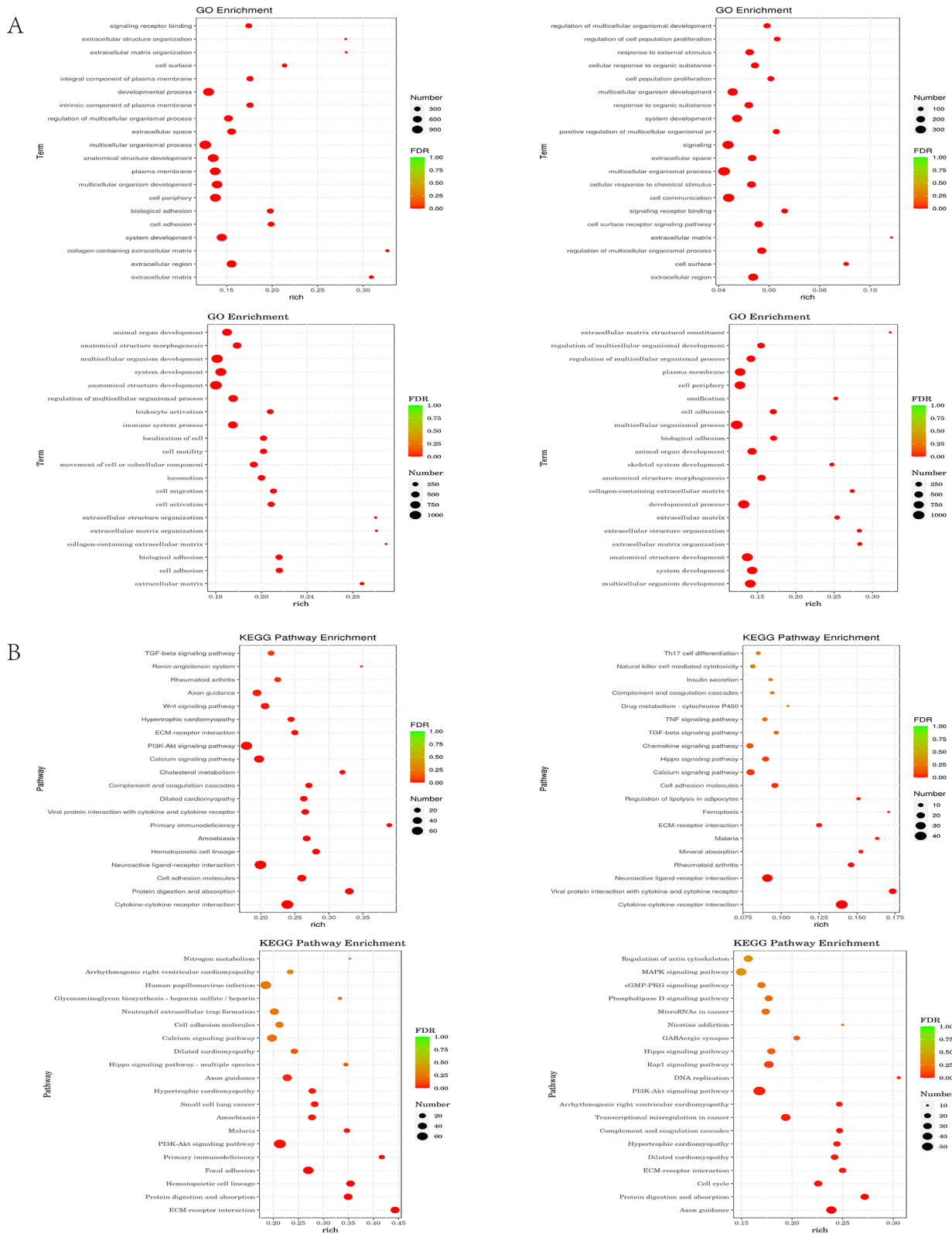


Fig. 2 (See legend on next page.)

(See figure on previous page.)

Fig. 2 GO/KEGG enrichment analysis of DEGs. **(A)** GO enriched bubble maps of DEGs obtained by comparison of different groups. **(B)** KEGG channel enrichment bubble maps of DEGs obtained by comparison of different groups. Tag the GO/KEGG entry to the right of the image. The horizontal coordinate is rich factor, which refers to the ratio of the number of DEGs enriched in GO/KEGG entries to the number of DEGs annotated; The greater the rich factor, the higher the degree of enrichment. Bubble color represents FDR value; FDR generally ranges from 0 to 1, and the closer it is to zero, the more significant the enrichment. Bubble size represents the number of genes enriched to GO/KEGG entries. The picture shows the top 20 items with the lowest FDR values of all items, i.e. the most significant enrichment. A represents spongy bone samples from OP patients, aa represents cortical bone samples from OP patients. B represents spongy bone samples of control group, and bb represents cortical bone samples of control group. Each group contained 6 samples

significantly down-regulated the transcription levels of Runx2, Opn and Ocn.

LncRNA AC003090.1 affects GSK-3 β and c-Myc signalling in hBMSCs through the miR-203a-3p/FOXP1 axis

We also examined the effects of AC003090.1 overexpression on the expression levels of GSK-3 β , β -catenin and c-Myc. Figure 5D and E show that the transcription and protein expression levels of β -catenin and c-Myc significantly increased in OI-cultured hBMSCs relative to in normal cultured hBMSCs. By contrast, the transcription and protein expression levels of GSK-3 β significantly decreased. The hBMSC OI group subjected to lentiviral vector infection with the empty plasmid was not significantly affected. Compared with transfection with hBMSC OI and hBMSC OI + lnc-NC, that with the AC003090.1-overexpressing plasmid significantly up-regulated the transcription and protein expression levels of β -catenin and c-Myc and inhibited those of GSK-3 β .

In addition, transfection with miR-203a-3p mimics and si-FOXP1 significantly up-regulated intracellular GSK-3 β transcription and protein expression levels but significantly inhibited β -catenin and c-Myc transcription and protein expression levels (Fig. 6B and C).

Discussion

The foundation of molecular biology begins with the transcription of genes from DNA into RNA. This phenomenon, in turn, leads to protein synthesis. RNA (collectively known as the transcriptome) is a complex genomic structure with coding and noncoding regions. It acts as an intermediary between genes and proteins. The study of the transcriptome is crucial for understanding genomic function, identifying the molecular composition of cells and understanding the causes and progression of diseases [28]. In this study, we employed NGS technology to perform transcriptome sequencing on six spongy bone and six cortical bone samples from postmenopausal patients with OP and six spongy bone and six cortical bone samples from postmenopausal control patients with low bone mass to obtain the transcriptome expression profiles of each sample. The DEGs between the two groups were analysed, and valuable information, which is conducive to further studies in the future, was obtained. The transcriptome sequencing results highlighted the differential expression of FOXP1, GSK3 β and β -catenin in the bone tissue of patients with OP, as well as the critical

role of GSK3 β / β -catenin signalling in the disease progression of OP. Our study also points to the inherent differences in cell activity and molecular mechanisms between human cortical and spongy bone tissues under physiological and pathological conditions. These variations include differences in cell motility, cell proliferation, immune microenvironment and responses to extracellular signals.

Bone can be classified as cortical or spongy depending on its microstructure. Cortical bone has a dense structure, and its units and plexiform flakes are arranged longitudinally. Spongy bones are loosely aligned with each other, and 20% of their volume comprises trabeculae in different directions, with the remaining space filled with bone marrow and fat. Studies have demonstrated that patients with type 2 diabetes mellitus have higher spongy bone density but lower cortical bone density than controls [29, 30]. Differences in composition may explain why Runx2, Opn and Ocn transcription levels in spongy bone are lower than those in cortical bone.

MACS is a simple, reliable and effective method for separating MSCs. BMSCs are a promising source of stem cells. In this study, MSCs were reliably isolated from human bone tissue through MACS by using CD105+/CD166+ surface markers. The specific expression of AC003090.1 in cortical and spongy bone tissues and bone-derived MSCs in patients with OP was higher than that in patients with low bone mass. Critically, AC003090.1 was specifically expressed in MSCs but not in non-MSCs. Moreover, its specific expression and change in MSCs were closely related to the progression of OP. In addition, compared with those in the control group, the expression of miR-203a-3p was significantly up-regulated and that of FOXP1 was significantly down-regulated in the cortical and spongy bone tissues and bone tissue-derived MSCs of patients with OP. The levels of AC003090.1 and FOXP1 in bone tissue showed predictive value for OP. Detecting the specific expression levels of AC003090.1 and FOXP1 in an expanded population cohort and blood samples and further analysing their predictive value for OP severity, fracture risk and drug effects are important.

FOXP1 can respond to various signals and control the ultimate fate of cells. The transcriptional inhibition mechanism of FOXP1 for p16INK4A is involved in the regulation of the fate of MSCs by FOXP1 [31]. Studies have shown that FOXP1 can up-regulate the transcription and

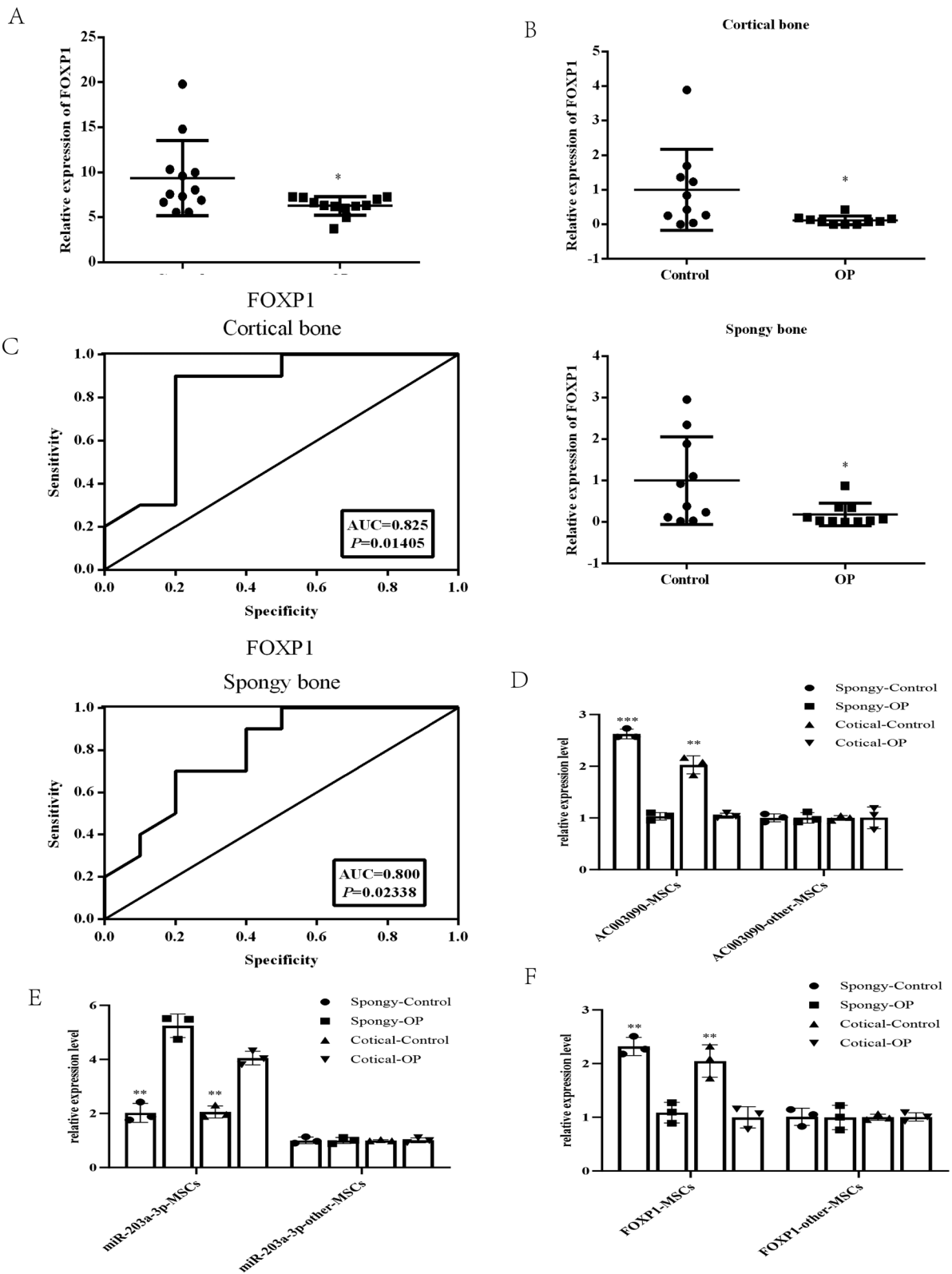
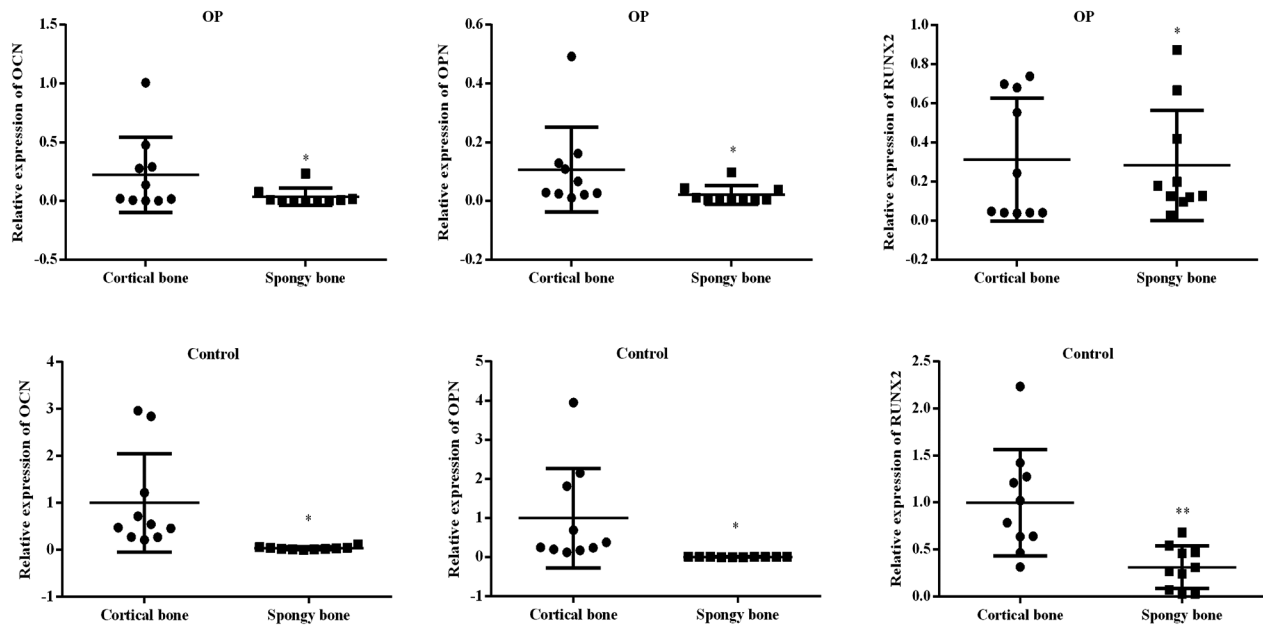


Fig. 3 (See legend on next page.)

(See figure on previous page.)

Fig. 3 The role of FOXP1, GSK3 β and β -catenin in OP. **(A)** The relative expression levels of FOXP1, GSK3 β and β -catenin in bone tissues of Control and OP groups obtained by high-throughput transcriptome sequencing. **(B)** The expression levels of AC003090.1, miR-203a-3p and FOXP1 in Cortical bone and Spongy bone tissues of OP group and Control group were detected by RT-qPCR. In OP group, $n=10$; Control group, $n=10$. **(C)** ROC curve analysis of FOXP1 level in bone tissue against OP. **(D)** RT-qPCR detection of MSCs and non-Mscs (Other) from Cortical bone and Spongy bone in Control group and OP group Expression levels of AC003090.1, miR-203a-3p and FOXP1 in cells. Magnetic activated cells sorted CD105 $^+$ /CD166 $^+$ into MSCs. $**P < 0.01$; $***P < 0.001$

A



B

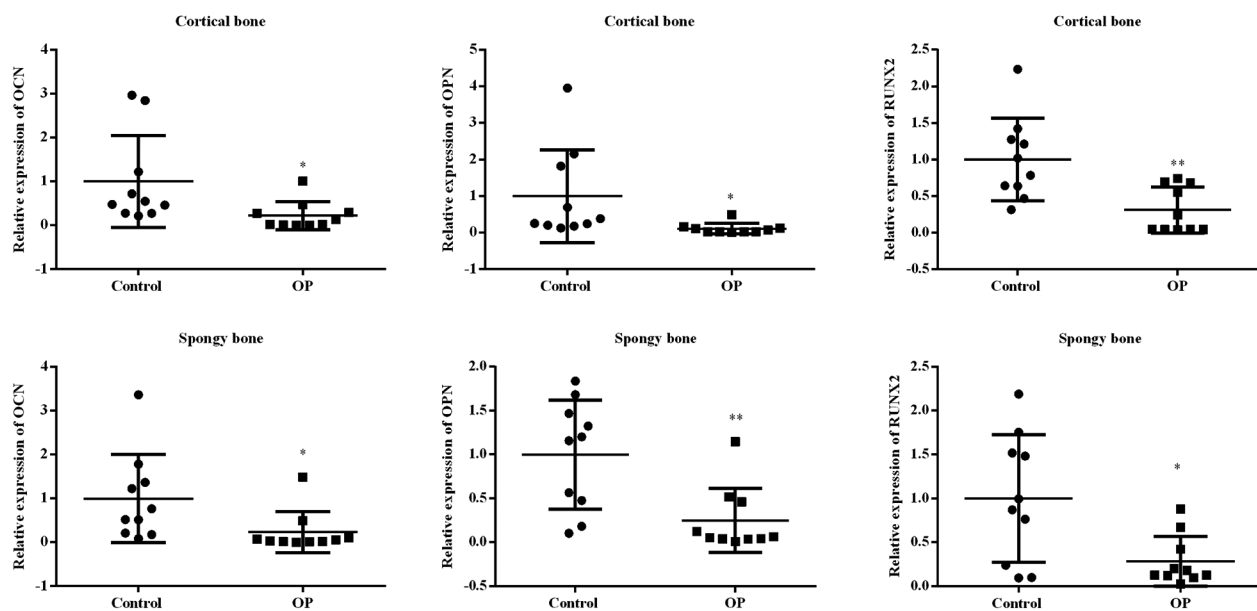


Fig. 4 Expression changes of Runx2, Opn and Ocn in bone tissue of OP patients. **(A, B)** Transcription levels of Runx2, Opn and Ocn in Cortical bone and Spongy bone tissues of OP group and Control group were detected by RT-qPCR. In OP group, $n=10$; Control group, $n=10$. $*P < 0.05$; $**P < 0.01$

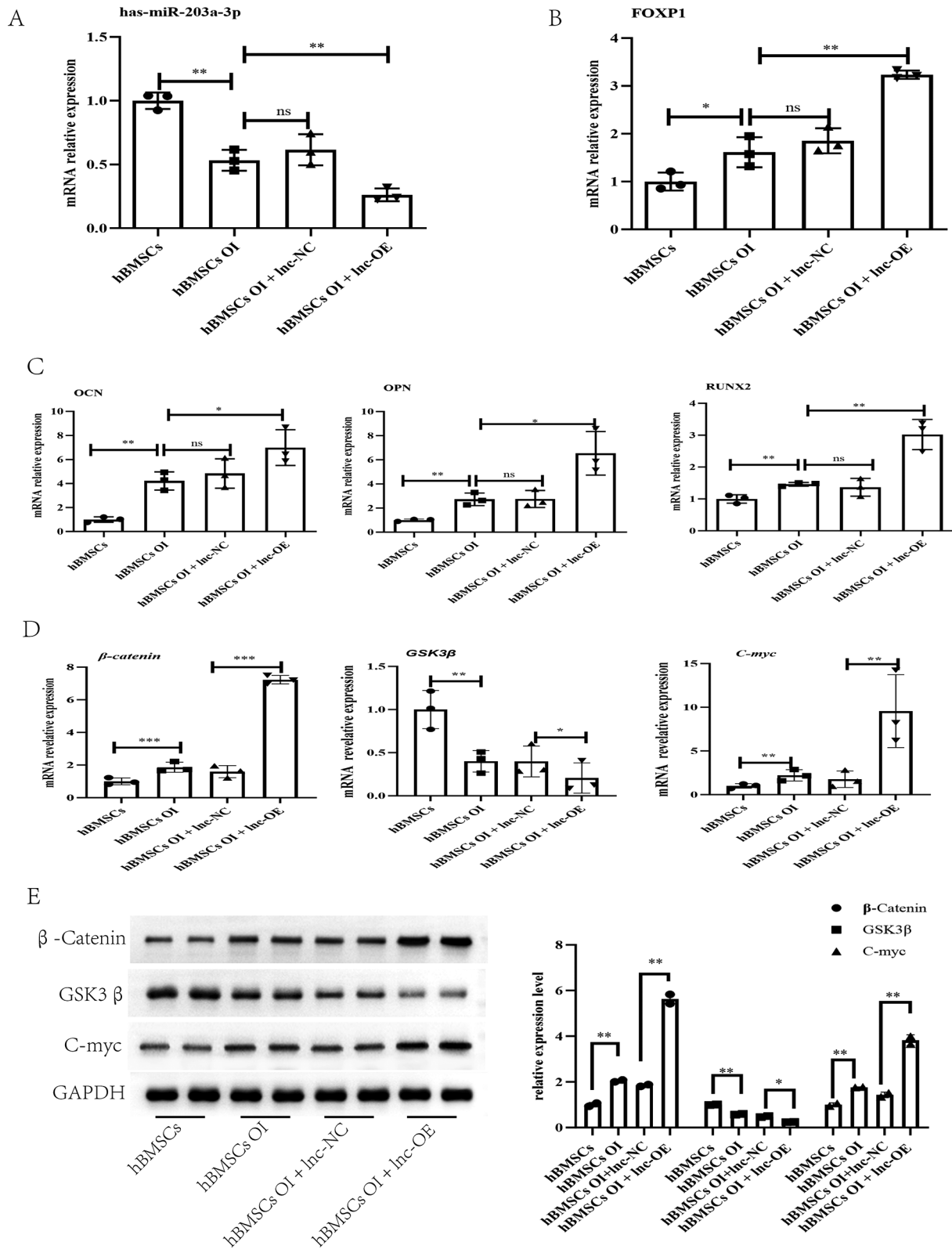


Fig. 5 (See legend on next page.)

(See figure on previous page.)

Fig. 5 Expression pattern specific changes of miR-203a-3p and FOXP1 during osteogenic differentiation of hBMSCs in vitro, and lncRNA AC003090.1 regulates their expression changes. **(A, B)** RT-qPCR was used to detect miR-203a-3p and FOXP1 mRNA levels of hBMSCs treated with different treatments. **(C)** RT-qPCR was used to detect Runx2, Opn and Ocn transcription levels of hBMSCs treated with different treatments. **(D)** RT-qPCR was used to detect the transcription levels of β -catenin, GSK-3 β and c-myc in different treated hBMSCs. **(E)** western blot detection of β -catenin, GSK-3 β and c-myc protein expression levels of hBMSCs treated with different treatments, compared with GAPDH. The data of hACMSCs group were normalized. ns, no significant difference; * $P < 0.05$; ** $P < 0.01$; *** $P < 0.001$

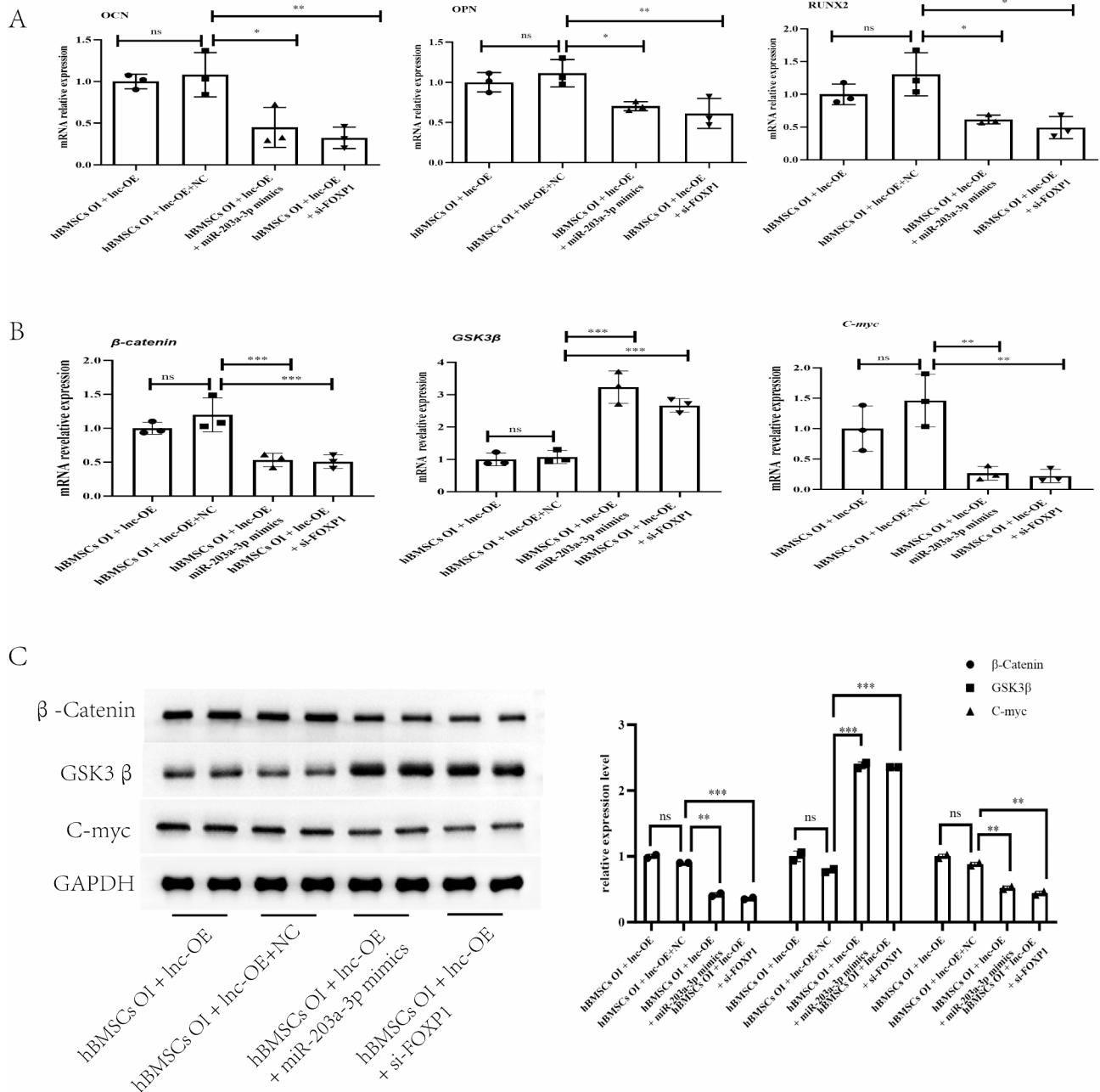


Fig. 6 LncRNA AC003090.1 affects GSK-3 β / β -catenin/c-myc signaling in hBMSCs through the miR-203a-3p/FOXP1 axis **(A)** RT-qPCR was used to detect Runx2, Opn and Ocn transcription levels of hBMSCs treated with different treatments. **(B)** RT-qPCR was used to detect the transcription levels of β -catenin, GSK-3 β and c-myc in different treated hBMSCs. **(C)** Western blot detection of β -catenin, GSK-3 β and C-myc protein expression levels of hBMSCs treated with different treatments, compared with GAPDH. The data of hBMSCs + lnc-OE group were normalized. ns, no significant difference; * $P < 0.05$; ** $P < 0.01$; *** $P < 0.001$

protein levels of β -catenin [32] and also activate c-Myc signalling in diffuse large B-cell lymphoma [33]. The deletion of Foxp1 leads to the dysregulation of c-Myc target gene expression [34]. lncRNA AC003090.1 may regulate β -catenin/c-Myc signalling through the up-regulation of FOXP1. In other words, lncRNA AC003090.1 can indirectly act on the transcription and expression levels of GSK-3 β , β -catenin and c-Myc by regulating the expression levels of miR-203a-3p and FOXP1 and ultimately regulate the osteogenic differentiation of hBMSCs. However, whether the effect of lncRNA AC003090.1 on GSK3 β / β -catenin/c-Myc has other regulatory mechanisms for myc signals still needs further exploration.

Conclusion

Given the regulatory effect of the lncRNA AC003090.1/miR-203a-3p/FOXP1 axis on GSK3 β / β -catenin signalling and the differential expression of GSK3 β and β -catenin in the bone tissue of patients with OP, we speculated that the downstream signalling pathway of the lncRNA AC003090.1/miR-203a-3p/FOXP1 axis participates in the osteogenic differentiation of MSCs and that OP progression involves GSK3 β / β -catenin signalling.

Supplementary Information

The online version contains supplementary material available at <https://doi.org/10.1186/s13018-025-05634-1>.

Supplementary Material 1

Author contributions

Huafeng Zhuang, Xuedong Yao and Youjia Xu wrote the main manuscript text and Yongjun Lin, Chengye Lin, Miao Zheng, and Yizhong Li prepared Figs. 1, 2, 3, 4, 5 and 6 and tables. All authors reviewed the manuscript.

Funding

This research was supported by Natural Science Foundation of Fujian Province(2021J01272).

Data availability

No datasets were generated or analysed during the current study.

Declarations

Ethics approval and consent to participate

The ethics committee of the Second Affiliated Hospital of Fujian Medical University approved the study after informed consent was obtained from all patients ([2019] the Second Affiliated Hospital of Fujian Medical University Ethics Review Letter No. (203)).

Competing interests

The authors declare no competing interests.

Author details

¹Department of Orthopedics, The Second Affiliated Hospital of Soochow University, Suzhou 215004, China

²Department of Orthopedics, The Second Affiliated Hospital of Fujian University, Quanzhou 362000, China

³Osteoporosis Clinical Center, The Second Affiliated Hospital of Soochow University, Suzhou 215004, China

Received: 19 December 2024 / Accepted: 20 February 2025

Published online: 07 April 2025

References

- Andersen MØ, Andresen AK, Hartvigsen J, Hermann AP, Sørensen J, Carreon LY. Vertebroplasty for painful osteoporotic vertebral compression fractures: a protocol for a single-center doubled-blind randomized sham-controlled clinical trial [J]. *VOPE2. J Orthop Surg Res.* 2024;19(1):813.
- Shen L, Yang H, Zhou F, Jiang T, Jiang Z. Risk factors of short-term residual low back pain after PKP for the first thoracolumbar osteoporotic vertebral compression fracture [J]. *J Orthop Surg Res.* 2024;19(1):792.
- Leeyaphan J, Rojjananukulpong K, Intarasompun P, Peerakul Y. Simple clinical predictors for making directive decisions in osteoporosis screening for women: a cross-sectional study [J]. *J Orthop Surg Res.* 2024;19(1):789.
- Feng Q, Zheng S, Zheng J. The emerging role of MicroRNAs in bone remodeling and its therapeutic implications for osteoporosis [J]. *Biosci Rep* 2018; 38.
- Khosla S, Oursler MJ, Monroe DG. Estrogen and the skeleton. *Trends Endocrinol Metab.* 2012;23:576–81.
- Wu S, Liu Y, Zhang L, et al. Genome-wide approaches for identifying genetic risk factors for osteoporosis [J]. *Genome Med.* 2013;5:44.
- Low SA, Kopecek J. Targeting polymer therapeutics to bone. *Adv Drug Deliv Rev.* 2012;64:1189–204.
- Migliorini F, Colarossi G, Eschweiler J, Oliva F, Driessen A, Maffulli N. Anti-resorptive treatments for corticosteroid-induced osteoporosis: a bayesian network meta-analysis [J]. *Br Med Bull.* 2022;143(1):46–56.
- Conti V, Russomanno G, Corbi G, Toro G, Simeon V, Filippelli W, Ferrara N, Grimaldi M, D'Argenio V, Maffulli N, Filippelli A. A polymorphism at the translation start site of the vitamin D receptor gene is associated with the response to anti-osteoporotic therapy in postmenopausal women from Southern Italy [J]. *Int J Mol Sci.* 2015;16(3):5452–66.
- Ducy P, Zhang R, Geoffroy V, et al. Osf2/Cbfa1: a transcriptional activator of osteoblast differentiation [J]. *Cell.* 1997;89:747–54.
- Valenti MT, Dalle CL, Mottes M. Osteogenic differentiation in healthy and pathological Conditions [J]. *Int J Mol Sci* 2016; 18.
- Li H, Liu P, Xu S, et al. FOXP1 controls mesenchymal stem cell commitment and senescence during skeletal aging [J]. *J Clin Invest.* 2017;127(4):1241–53.
- Sun Y, et al. Osteoblast-targeting-peptide modified nanoparticle for siRNA/microRNA delivery. *ACS Nano.* 2016;10:5759–68.
- Bao X, Liu C, Liu H, Wang Y, Xue P, Li Y. Association between polymorphisms of glucagon-like peptide-1 receptor gene and susceptibility to osteoporosis in Chinese postmenopausal women [J]. *J Orthop Surg Res.* 2024;19(1):869.
- Huang F, Wang Y, Liu J, Cheng Y, Zhang X, Jiang H. Asperuloside alleviates osteoporosis by promoting autophagy and regulating Nrf2 activation [J]. *J Orthop Surg Res.* 2024;19(1):855.
- Zeng X, Dong Q, Liu Q, Tan WJ, Liu XD. lncRNA HOTTIP facilitates osteogenic differentiation in bone marrow mesenchymal stem cells and induces angiogenesis via interacting with TAF15 to stabilize DLX2 [J]. *Exp Cell Res.* 2022;417(2):113226.
- Spreitzer E, Alderson TR, Bourgeois B, Eggenreich L, Habacher H, Brahmersdorfer G, Pritisanac I, Sanchez-Murcia PA, Madl T. FOXO transcription factors differ in their dynamics and intra/intermolecular interactions [J]. *Curr Res Struct Biol.* 2022;4:118–33.
- Shen W, Sun B, Zhou C, Ming W, Zhang S, Wu X. CircFOXP1/FOXP1 promotes osteogenic differentiation in adipose-derived mesenchymal stem cells and bone regeneration in osteoporosis via miR-33a-5p [J]. *J Cell Mol Med.* 2020;24(21):12513–24.
- Li S, Wang Y, Zhang Y, Lu MM, Demayo FJ, Dekker JD, Tucker PW, Morrisey EE. Foxp1/4 control epithelial cell fate during lung development and regeneration through regulation of anterior gradient 2 [J]. *Development.* 2012;139(14):2500–9.
- Huynh NP, Anderson BA, Guilak F, Mcalinden A. Emerging roles for long noncoding RNAs in skeletal biology and disease [J]. *Connect Tissue Res.* 2017;58(1):116–41.
- Oliviero A, Della Porta G, Peretti GM, Maffulli N. MicroRNA in osteoarthritis: pathophysiology, diagnosis and therapeutic challenge [J]. *Br Med Bull.* 2019;130(1):137–147. <https://doi.org/10.1093/bmb/ldz015>. Erratum in: *Br Med Bull.* 2022;144(1):90.
- Gargano G, Asparago G, Spiezia F, Oliva F, Maffulli N. Small interfering RNAs in the management of human osteoporosis [J]. *Br Med Bull.* 2023;148(1):58–69.

23. Zhu G, Zeng C, Qian Y, Yuan S, Ye Z, Zhao S, Li R. Tensile strain promotes osteogenic differentiation of bone marrow mesenchymal stem cells through upregulating lncRNA-MEG3 [J]. *Histol Histopathol*. 2021;36(9):939–46.
24. Tang JZ, Zhao GY, Zhao JZ, Di DH, Wang B. LncRNA IGF2-AS promotes the osteogenic differentiation of bone marrow mesenchymal stem cells by sponging miR-3,126-5p to upregulate KLK4 [J]. *J Gene Med*. 2021;23(10):e3372.
25. Huafeng Zhuang X, Yao A, Wang J, Li M, Zheng Y, Dong Y, Xu Y, Li, Lin Y. LncRNA AC003090.1 mediates miR-203a-3p/FOXP1 Axis to promote the osteogenic differentiation of human bone marrow mesenchymal stem cells [J]. *J Biomed Nanotechnol*. 2024;20:207–15.
26. Florea L, Song L, Salzberg SL. Thousands of exon skipping events differentiate among splicing patterns in sixteen human tissues [J]. *F1000Res*. 2013;2:188.
27. Trapnell C, Roberts A, Goff L, Pertea G, Kim D, Kelley DR, Pimentel H, Salzberg SL, Rinn JL, Pachter L. Differential gene and transcript expression analysis of RNA-seq experiments with tophat and cufflinks [J]. *Nat Protoc*. 2012;7(3):562–78.
28. Wang B, Kumar V, Olson A, Ware D. Reviving the transcriptome studies: an insight into the emergence of Single-Molecule transcriptome sequencing [J]. *Front Genet*. 2019;10:384.
29. Ho-Pham LT, Chau PMN, Do AT, Nguyen HC, Nguyen TV. Type 2 diabetes is associated with higher trabecular bone density but lower cortical bone density: the Vietnam osteoporosis study [J]. *Osteoporos Int*. 2018;29(9):2059–67.
30. Hsu PY, Tsai MT, Wang SP, Chen YJ, Wu J, Hsu JT. Cortical bone morphological and trabecular bone microarchitectural changes in the mandible and femoral neck of ovariectomized rats [J]. *PLoS ONE*. 2016;11(4):e0154367.
31. Li H, Liu P, Xu S, Li Y, Dekker JD, Li B, Fan Y, Zhang Z, Hong Y, Yang G, Tang T, Ren Y, Tucker HO, Yao Z, Guo X. FOXP1 controls mesenchymal stem cell commitment and senescence during skeletal aging [J]. *J Clin Invest*. 2017;127(4):1241–53.
32. Wang C, Tan C, Wen Y, Zhang D, Li G, Chang L, Su J, Wang X. FOXP1-induced LncRNA CLRN1-AS1 acts as a tumor suppressor in pituitary prolactinoma by repressing the autophagy via inactivating Wnt/beta-catenin signaling pathway [J]. *Cell Death Dis*. 2019;10(7):499.
33. Dekker JD, Park D, Shaffer AL 3rd, Kohlhammer H, Deng W, Lee BK, Ippolito GC, Georgiou G, Iyer VR, Staudt LM, Tucker HO. Subtype-specific addiction of the activated B-cell subset of diffuse large B-cell lymphoma to FOXP1 [J]. *Proc Natl Acad Sci U S A*. 2016;113(5):E577–86.
34. Felce SL, Anderson AP, Maguire S, Gascoyne DM, Armstrong RN, Wong KK, Li D, Banham AH. CRISPR/Cas9-Mediated Foxp1 Silencing restores immune surveillance in an immunocompetent A20 lymphoma model [J]. *Front Oncol*. 2020;10:448.

Publisher's note

Springer Nature remains neutral with regard to jurisdictional claims in published maps and institutional affiliations.